Influence of polylactide coating stereochemistry on mechanical and in vitro degradation properties of porous bioactive glass scaffolds for bone regeneration

Uppstu, Peter; Engblom, Simon; Inkinen, Saara; Hupa, Leena; Wilen, Carl-Eric

Published in:
Journal of Biomedical Materials Research Part B: Applied Biomaterials

DOI:
https://doi.org/10.1002/jbm.b.35328

Published: 01/01/2024

Document Version
Final published version

Document License
CC BY

Received: 8 April 2023 | Revised: 25 August 2023 | Accepted: 7 September 2023

DOI: 10.1002/jbm.b.35328

RESEARCH ARTICLE

Society For Biomaterials | WILEY

Influence of polylactide coating stereochemistry on mechanical and in vitro degradation properties of porous bioactive glass scaffolds for bone regeneration

Peter Uppstu[1] | Simon Engblom[1] | Saara Inkinen[1,2] | Leena Hupa[1] | Carl-Eric Wilén[1]

[1]Laboratory of Molecular Science and Technology, Faculty of Science and Engineering, Åbo Akademi University, Turku, Finland

[2]Nordic Catalyst e.U., Vienna, Austria

Correspondence
Peter Uppstu, Laboratory of Molecular Science and Technology, Faculty of Science and Engineering, Åbo Akademi University, Turku, Finland.
Email: peter.uppstu@abo.fi

Funding information
Stiftelsen för Åbo Akademi; Svenska Kulturfonden; Tekniikan Edistämissäätiö

Abstract

The mechanical properties of polylactide stereocomplexes (PLA SC) have been primarily studied through tensile testing, with inconsistent results, and the compressive properties of PLA SC compared to homocrystalline or amorphous PLA remain poorly understood. In this study, we coated porous bioactive glass 13–93 scaffolds with amorphous, homocrystalline, or stereocomplex PLA to investigate their mechanical and degradation properties before and after immersion in simulated body fluid. The glass scaffolds had interconnected pores and an average porosity of 76%. The PLA coatings, which were 10–100 μm thick and approximately 3% of the glass scaffold mass, covered the glass to a large extent. The compressive strength and toughness of all PLA-coated scaffolds were significantly higher than those of uncoated scaffolds, with approximately a fourfold increase before immersion and a twofold increase after immersion. The compressive strength and toughness of PLA SC-coated scaffolds were similar to those of scaffolds with homocrystalline PLA coating, and significantly higher than for scaffolds with amorphous PLA coating. All PLA coatings moderated the initial pH increase caused by the glass, which could benefit surrounding cells and bone tissue in vivo after implantation.

KEYWORDS
bioactive glass, compressive testing, polylactide stereocomplex, scaffold, simulated body fluid

1 | INTRODUCTION

Polylactide (PLA) is a thermoplastic poly(α-hydroxyester) studied for various biomedical applications, including tissue regeneration and drug release.[1–3] It is widely used in orthopedic applications in porous scaffolds and composite implants both as a continuous and a non-continuous phase.[4,5] In orthopedic fixation, PLA is used clinically for example in plates, screws, and pins.[6]

The properties of PLA can be modified by altering its molecular weight, structure, and stereochemistry. Structural modifications include introducing branching, cross-linking, or tethering functional groups via copolymerization.[5] As the lactide dimer contains two chiral carbon atoms, it can exist in three forms: L,L-, D,D-, and D,L-lactide. The ability of PLA to crystallize and, therefore, its thermal and mechanical properties depend on the stereoform of the monomers. Crystallization generally occurs in PLA with an optical purity of at least 72%–75%, while PLA closer to a racemic mixture of the two forms remains amorphous.[7,8]

By blending poly(L-lactide) (PLLA) with poly(D-lactide) (PDLA), one can form stereocomplex crystallites with strong stereoselective

association between PLLA and PDLA.[9,10] Stereocomplex PLA (PLA SC) crystallites consist of PLLA and PDLA at a 1:1 ratio. PLA SC can be formed in the presence of chains or chain segments of PLLA and PDLA in solution, by cooling from melt, during polymerization, or during hydrolytic degradation.[11] Especially for PLA with a molecular weight higher than 100,000 g/mol, stereocomplex crystallization can be enhanced with synthesis of stereoblock-type PLA with blocks of PLLA and PDLA within the same chain.[12]

PLA SC has a higher melting point (220–230°C) than homocrystalline PLA (170–180°C)[13] and is hydrolytically[14–16] and thermally[17] more stable. However, its hydrolysis forms more acidic degradation products,[18] which may affect bone regeneration negatively.[1] Composites with bioactive glass neutralize acidic degradation products.[19,20] The degradation products of polyesters may even be used as positive irritation to stimulate the formation of growth factors for enhanced bone formation.[21–24]

PLA SC is often reported to have enhanced mechanical properties compared to isomerically pure PLLA or PDLA.[8,11,25,26] Although some studies support these claims,[27,28] others suggest similar or even inferior[29–31] tensile strength for stereocomplexes compared to other PLA forms. The compressive properties of PLA SC have not yet been extensively investigated. In one study, PLA with a small fraction of stereocomplex crystallites exhibited greater compressive strength than isomerically pure PLLA.[32] In other studies, PLLA and PDLA blended with D-mannitol[33] or ethylene-glycidyl methacrylate copolymer[34] exhibited higher compressive strength than pure PLLA. However, in these papers, the materials were studied as foams with different porosities for PLA SC compared to PLLA, complicating direct comparisons of material properties.

Scaffolds for bone regeneration are typically composed of biodegradable materials, such as PLA, processed into porous structures. When a scaffold is implanted into a bone defect, cells enter its pores, adhere to the pore walls, and generate new tissue. As the tissue grows, the scaffold degrades, ideally allowing the defect site to be filled with new bone as the scaffold completely degrades.[2] Although PLA is biocompatible, it lacks biologically active cues, and it is frequently combined with bioactive glasses for improved tissue growth.[6]

Bioactive glasses 45S5 and S53P4 can be favorably used to regenerate bone tissue.[35,36] They are clinically used as granules, pastes, plates, and discs. Despite intense research on creating porous three-dimensional (3D) scaffolds based on these glasses, no clinical products exist yet.[37] Several methods have been proposed for producing porous scaffolds from melt-derived bioactive glasses, including sintering of glass particles in a mold,[38,39] solid free-form fabrication techniques,[40,41] and the foam replication technique.[42] Each of these methods require a sintering step to consolidate the glass particles into the desired porous structure. The strong crystallization tendency during thermal treatment poses challenges when manufacturing porous scaffolds of 45S5 and S53P4. Extensive research has been conducted to adjust the composition of bioactive glasses to better suit various hot working processes. Bioactive glass 13–93 was found to allow versatile hot working[43,44] and is suitable for producing porous non-crystallized scaffolds for tissue regeneration.[39,45]

Low compressive strength and fracture toughness are main limitations of porous bioactive glass scaffolds.[46,47] Although 3D bioactive glass scaffolds have been designed for high compressive strength, this is generally achieved by compromising porosity, pore size, or pore interconnectivity.[48] The mechanical properties of bioactive glass scaffolds can be improved by coating them with biodegradable synthetic or naturally occurring polymers, such as PLA, poly(lactide-co-glycolide) (PLGA), polycaprolactone (PCL), poly(3-hydroxybutyrate) (P3HB), gelatin, silk, alginate, collagen, or chitosan.[49–51] Bioactive glass-based scaffolds produced with the foam replication method and coated with polymers typically exhibit compressive strength values of 1 MPa or below.[49]

In this study, we examined the impact of PLA coating morphology on the compressive and degradation properties of porous bioactive glass 13–93 scaffolds in a clinically relevant setting for bone regeneration, both before and after immersion in simulated body fluid (SBF). We used three types of PLA coatings with distinct morphologies: amorphous poly(D,L-lactide) (PDLLA), homocrystalline PLLA, and a 1:1 stereocomplex mixture of PLLA and PDLA. Pore morphology, total porosity, and the mass and thickness of the scaffold coatings were measured, and the polymer coatings were analyzed with differential scanning calorimetry (DSC). We immersed the scaffolds in SBF for 0, 2, 4, 6, or 10 weeks and measured mass loss, water absorption, pH, and compressive properties at each time point. The findings in this study provide insights into the selection of PLA-based coating stereochemistry for biomedical implants, with the aim to optimize their mechanical properties and degradation behavior.

2 | MATERIALS AND METHODS

2.1 | Materials

Medical-grade L-lactide, D-lactide, and D,L-lactide monomers (Corbion, Gorinchem, the Netherlands) were used to polymerize PLA. Bioactive glass 13–93, with a nominal composition of 53 SiO_2, 6 Na_2O, 12 K_2O, 5 MgO, 20 CaO, and 4 P_2O_5 (all in wt %), was prepared by mixing Belgian quartz sand with analytical-grade reagents Na_2CO_3, K_2CO_3, MgO, $CaCO_3$, and $CaHPO_4{\cdot}2(H_2O)$. The batch was melted in a platinum crucible at 1360°C for 3 h, cast, annealed, crushed, and remelted to ensure homogeneity. The annealed glass block was crushed, milled, and sieved to obtain a size fraction of 32–45 µm. All other chemicals used in this study were of analytical or equivalent grade.

2.2 | Polymerization

PLLA, PDLA, and racemic PDLLA were synthesized by ring-opening polymerization, following a previously reported procedure.[20] Briefly, 0.1 mol % stannous octoate was used as an initiator, and 1-decanol as a co-initiator. The polymerization was conducted in 200 g batches under an argon atmosphere for 3 h at 150°C with initial stirring. The polymer was subsequently dissolved in dichloromethane and carefully precipitated in ethanol.

2.3 | Production of glass scaffolds by foam replication

Polyethylene glycol (35,000 g/mol) was dissolved in ethanol at a concentration of 5 wt % at 40°C. Bioactive glass 13–93 particles (7.5 wt % compared to ethanol) were dispersed into the solution in a ball mill for 30 min. After milling, the mean particle size was 20.2 μm as measured with laser light scattering. Cylindrical PU foams (20 mm height, 18 mm diameter, and 15 pores per inch) were immersed in the slurry. To ensure full penetration of the slurry into the foam, the foams were manually compressed and released while still submerged in the slurry. Excess slurry was carefully removed with compressed air when removing the foams from the slurry. The slurry-coated foams were dried at room temperature (RT) for a minimum of 3 days to create green bodies. To burn out the polymer and sinter the glass, the green bodies were heated according to the following procedure: heating from RT to 300°C at 1°C min^{-1}, heating to 450°C at 0.8°C min^{-1}, 30 min hold at 450°C, heating to 670°C at 0.8°C min^{-1}, and 120 min hold at 670°C, after which the scaffolds were slowly cooled in the furnace to RT. The sintered glass scaffolds were stored in a desiccator until further use. Figure 1 shows the PU sacrificial foam before coating with the slurry, the slurry-coated green body, and the bioactive glass scaffold after sintering.

2.4 | Coating of glass scaffolds with PLA

The glass scaffolds were coated with PLA using a dip-coating technique. The stereocomplex solutions were prepared by dissolving 0.75 g PDLA and 0.75 g PLLA in 25 g $CHCl_3$ for a polymer concentration of 6 wt %. For the PDLLA and PLLA solutions, 1.5 g of either PDLLA or PLLA was dissolved in 25 g $CHCl_3$. The dry glass scaffolds were immersed in the polymer solution in beakers for 3 min, during which the beakers were placed in a vacuum oven, and the air pressure was reduced to 600 mbar for 60 s to remove bubbles from the scaffolds. The scaffolds were removed from the solution and gently blown with compressed air to open clogged pores. The polymer-coated scaffolds were dried overnight in a fume hood at RT, after which they were further dried overnight at RT at <50 mbar pressure. After coating and drying, the scaffolds were weighed again to determine the mass of the polymer coating.

The crystallinity of the polymer was increased by heat-treating the scaffolds. Preliminary tests were conducted to determine the optimal conditions for stereocomplex formation. We found that heat treatment at temperatures equal to or exceeding the melt temperature of homocrystalline PLA at 180°C significantly enhanced stereocomplex formation compared to lower temperatures, which is in agreement with previous studies.[31,52] Consequently, the scaffolds were heated under nitrogen atmosphere at 180°C for 60 min.

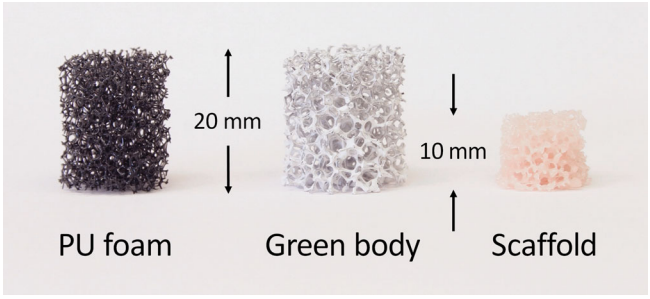

FIGURE 1 A polyurethane foam, a green body, and a final sintered bioactive glass scaffold. The figure illustrates the volume decrease of the scaffolds during the sintering step.

2.5 | Characterization of microstructure

The microstructure of the glass scaffolds was analyzed with μ-CT (SkyScan 1072, SkyScan, Kontich, Belgium). Cross-sections of scaffolds were analyzed by SEM (LEO Gemini 1530, Carl Zeiss, Oberkochen, Germany) at a magnification of ×30. To preserve the macrostructure, scaffolds were embedded in epoxy resin before being ground and polished to expose the cross-section of the scaffold. EDX analysis (UltraDry X-ray detector, Thermo Fisher Scientific, WI, USA) was used to identify the reaction layers of the glass. The coverage of coating and reaction layers on the glass surface was estimated visually from the SEM images.

2.6 | In vitro degradation

The in vitro degradation properties of the polymer-coated scaffolds were studied in SBF using a 1:30 ratio of scaffold (in g) to SBF (in mL). SBF was prepared using a standard procedure.[53] The scaffolds, immersed in plastic containers, were placed in a shaking incubator at 100 rpm at 37°C for various durations (2, 4, 6, or 10 weeks). The 0-week scaffolds were analyzed without immersion in SBF. The pH of the immersion solution was measured every week for at least three parallel scaffolds. The solution for all scaffolds was replenished weekly to fresh SBF. The ratio between scaffold mass and SBF volume was chosen based on the low surface area of the scaffolds, the relatively slow reactivity of the 13–93 glass, and on the weekly replenishing of the SBF solution.

A total of eight parallel scaffolds were immersed in SBF for each time point and coating type. Five of the eight parallel scaffolds were randomly chosen for compressive testing. The remaining three scaffolds were superficially dried using tissue paper, weighed, freeze-dried, weighed again, and subjected to other analyses. The percentage of water absorption was calculated as the amount of water that was lost during scaffold drying divided by the dried mass after immersion. The mass loss was determined as the difference between the dry mass before and after immersion, divided by the pre-immersion dry mass.

2.7 | Compressive testing

Compression tests were performed using an L&W Crush Tester (Lorentzen & Wettre, Stockholm, Sweden). Five parallel scaffolds were

compressed along their axis at a rate of 2 mm/min. The 0-week scaffolds were compressed in their dry state, while the 2–10-week scaffolds were compressed in their wet state immediately after removal from the SBF. The toughness of each scaffold was estimated as the strain energy density calculated from the integral of the stress–strain curve up to 33% strain. The compressive strength was identified as the peak value up to 33% strain. The threshold level of 33% was chosen to allow for sufficient data to be collected to account for the slight variation in the structure and shape between parallel scaffolds.

2.8 | Analysis of the polymer coating

The thermal properties of the polymer coating were analyzed using DSC with a DSC Q1000 (TA Instruments) under a nitrogen atmosphere. The samples were heated from 10 to 250°C at a rate of 10°C min^{-1}. The glass transition temperature (T_g) was identified as the half-height value, and the melting temperature (T_m) was determined as the maximum value of the endothermic peak. As the samples for DSC analysis mainly consisted of bioactive glass with only a small, undefined amount of PLA, specific melting enthalpies could not be calculated. Thermal analysis was conducted in triplicate for all coated 0-week and 10-week scaffolds.

The number average molecular weight (M_n) and weight average molecular weight (M_w) of the polymers were measured using gel permeation chromatography (GPC) with an LC-10ATVP HPLC pump (Shimadzu Corporation, Kyoto Japan), an AM GPC Gel 10 µm linear column (Mentor, Ohio, USA), and a Sedex 85 light scattering detector (Sedere, Alfortville, France). Polystyrene samples with narrow molecular weight distributions were used as standards.

2.9 | Statistical analysis

Statistical analysis was performed using SAS 9.4 software (SAS Institute). Analysis of variance was conducted with linear and linear mixed models. Post hoc tests were employed to explore differences among the means of the coating groups while accounting for other explanatory factors in the model. In the statistical analysis of the pH of the immersion solution, the individual scaffold number was designated as a random factor to take into account multiple measurements per individual scaffold over time. Differences were considered statistically significant at p values <.05.

3 | RESULTS

3.1 | Structural analysis of the glass scaffolds

The foam replication method, using sacrificial polyurethane templates, produced scaffolds with high pore interconnectivity and an architecture resembling trabecular bone. The scaffolds had an average porosity of 76%. Figure 2 displays the pore size distribution of uncoated and coated glass scaffolds, measured with µCT as the average of two parallel scaffolds. Pore sizes were highly variable, predominantly between 100 and 1700 µm. On average, pore sizes of uncoated scaffolds were smaller than those of coated scaffolds. Coated scaffolds had fewer pores in the 50–1000 µm range and more pores in the 1300–1700 µm range compared to uncoated scaffolds. The cylindrical-shaped sintered glass scaffolds had an average height of 9.9 mm and an average mass of 746 mg.

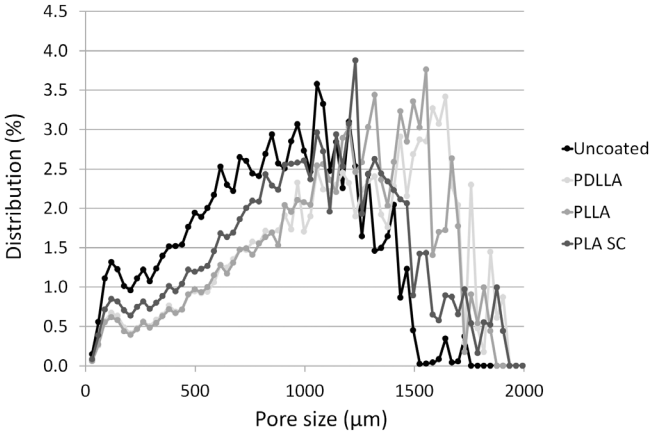

FIGURE 2 Pore size distribution of uncoated and coated bioactive glass scaffolds.

TABLE 1 Molecular weights and dispersity ($Đ$) of PLA polymers used in the coating of the 13–93 bioactive glass scaffolds as measured with GPC, and the average coating mass as a percentage of glass scaffold mass.

	M_n	M_w	$Đ$	Mass of coating (%)
PDLLA	33,000	56,000	1.7	2.6
PLLA	28,000	48,000	1.7	3.4
PDLA	26,000	43,000	1.7	3.2

Abbreviations: GPC, gel permeation chromatography; PDLLA, amorphous poly(D,L-lactide); PDLA, poly(D-lactide); PLA, polylactide; PLLA, poly(L-lactide).

3.2 | Properties of the polymer coating

Table 1 presents the molecular weight data of the precipitated and dried PDLLA, PLLA, and PDLA. The average mass of polymer coatings was approximately 3% of the glass scaffold mass for all coatings.

According to SEM analysis (Figure 6), the pores within the coated glass scaffolds were mostly covered with PLA coating, leaving approximately 20% of the glass surfaces uncoated. Most of the coating was located in the inner parts of the scaffolds, with less coating near the glass scaffold edges. The coating thickness varied, typically ranging between 10 and 100 µm.

DSC heating graphs for the scaffold coatings are shown in Figure 3, and thermal transition data from the DSC experiments is

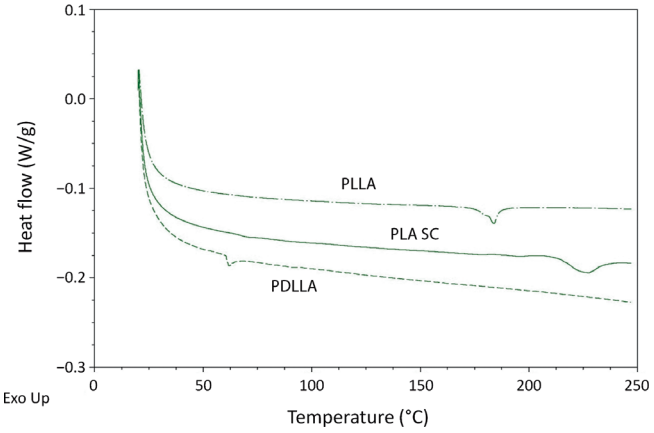

FIGURE 3 DSC curves illustrating phase transitions of PDLLA, PLLA, and PLA SC coatings before immersion in SBF. DSC, differential scanning calorimetry; PDLLA, amorphous poly(D,L-lactide); PLA, polylactide; PLLA, poly(L-lactide); SBF, simulated body fluid.

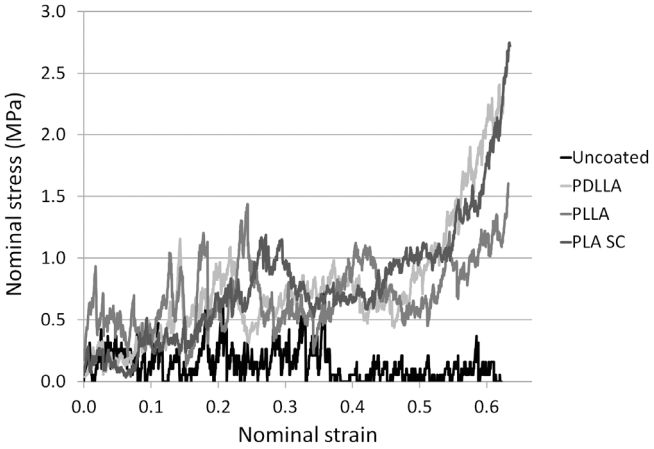

FIGURE 4 Compressive stress–strain graphs for 0-week scaffolds.

TABLE 2 Thermal transition points of PDLLA, PLLA, and PLA SC before immersion and after 10 weeks of immersion in SBF presented as averages ± SD.

Coating	Transition	0 weeks (°C)	10 weeks (°C)
PDLLA	T_g	60.5 ± 0.3	56.8 ± 0.7
PLLA	T_g	68.0 ± 0.5	68.3 ± 0.2
PLA SC	T_g	67.6 ± 0.6	71.5 ± 0.5
PLLA	T_m	183.2 ± 0.9	173.1 ± 0.7
PLA SC	T_m	225.2 ± 1.2	227.1 ± 0.7

Abbreviations: PDLLA, amorphous poly(D,L-lactide); PDLA, poly(D-lactide); PLA, polylactide; PLLA, poly(L-lactide); PLA SC, polylactide stereocomplexes; SBF, simulated body fluid.

summarized in Table 2. The thermal transition peaks in DSC were weak because the analyses were performed with crushed scaffolds, which primarily consisted of bioactive glass 13–93 (which does not undergo any transitions within the temperature range of the analyses) and only approximately 3 wt % of polymer. Distinct transitions in DSC occurred at the T_g for PDLLA (amorphous), the T_m for PLLA (homocrystalline), and the T_m for PLA SC (stereocomplex). Additionally, PLLA and PLA SC exhibited glass transitions, indicating their semi-crystalline nature. Besides the transitions reported in Table 2, melting of homocrystals for PLA SC scaffolds was detected in one 10-week scaffold, with a melting peak value of 176.1°C. Furthermore, there was a minor cold crystallization peak for all 10-week PLLA scaffolds at approximately 93°C.

3.3 | Compressive properties

Compressive stress–strain curves of representative 0-week scaffolds are presented in Figure 4. The toughness expressed as strain energy density during the initial 33% compression of the scaffold height before and after immersion in SBF is illustrated in Figure 5A. During compressive testing, all scaffolds experienced progressive failure, as parts of the scaffolds were continuously torn off, rather than the whole scaffold cracking at once. The size of the torn-off parts was smaller for uncoated scaffolds compared to coated scaffolds.

The toughness of the uncoated scaffolds remained unchanged from the dry state before immersion through the 10-week-long immersion in SBF ($p = .88$). In contrast, the toughness of all coated scaffolds was significantly higher before immersion than after immersion ($p < .0001$). Before immersion, no statistically significant difference was found between the three coatings ($p = .89$). The toughness of coated scaffolds remained constant throughout the immersion period, with no change from the 2-week time point until the 10-week time point ($p = .96$). After 2–10 weeks of immersion in SBF, the toughness of PLA SC-coated ($p = .0012$) and PLLA-coated ($p = .042$) scaffolds was significantly higher than that of PDLLA-coated scaffolds. The difference between PLA SC and PLLA coatings was not statistically significant ($p = .41$).

Figure 5B displays the compressive strength before and after immersing the scaffolds in SBF. The peak compressive strength in the dry state before immersion was 0.74 MPa for uncoated scaffolds, 1.46 MPa for PDLLA, 1.56 MPa for PLLA, and 1.68 MPa for PLA SC. After immersion, the compressive strength was slightly higher for coated scaffolds than for uncoated scaffolds.

3.4 | In vitro bioactivity and degradation properties

Figure 6 shows cross-sectional SEM images of 10-week scaffolds which were dried and cast in epoxy resin. Reaction layers of the bioactive glass, that is, silica-rich and calcium phosphate (CaP) layers, were visible for all scaffolds after immersion in SBF.

The abundance and thickness of the CaP reaction layer increased with immersion time in SBF. For uncoated scaffolds, a prominent CaP

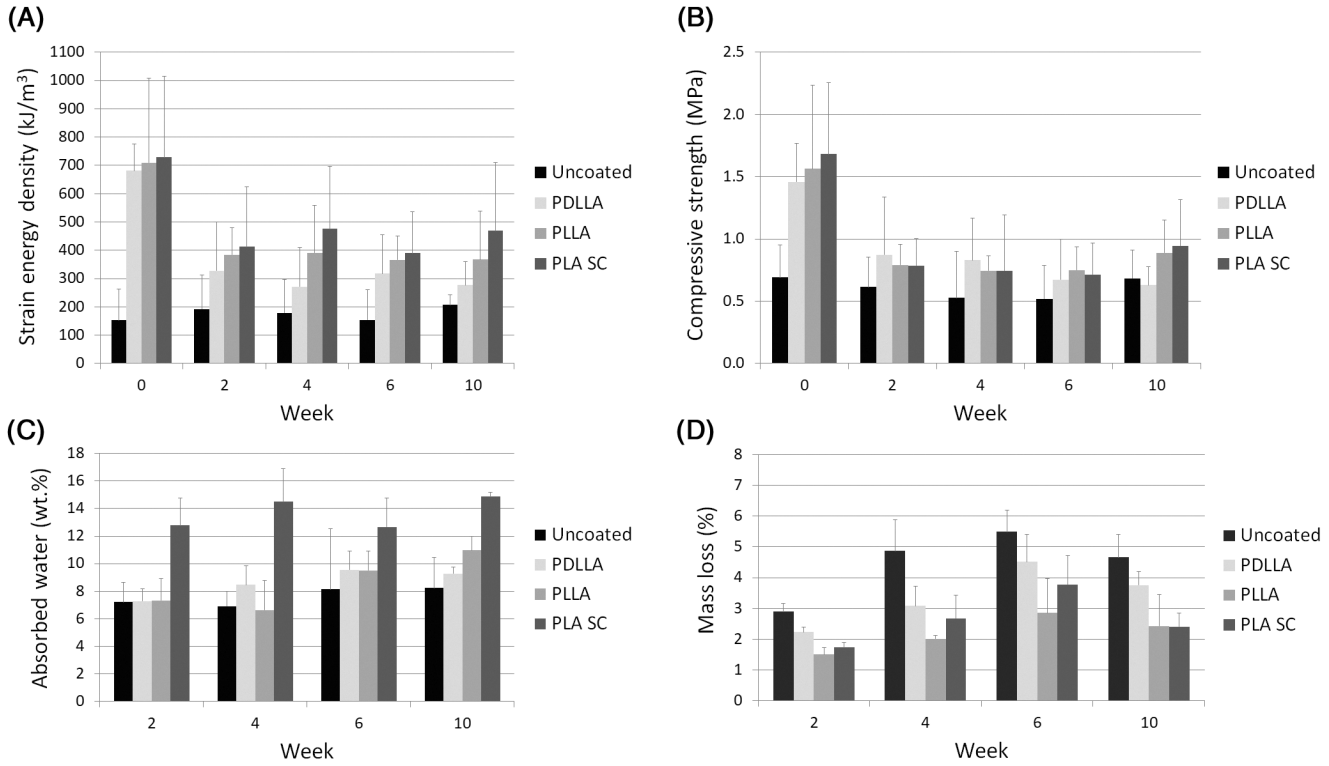

FIGURE 5 Properties of uncoated and coated glass scaffolds. (A) Strain energy density before and after immersion in simulated body fluid (SBF), calculated as the integral of the stress–strain curve for the initial 33% compression. (B) Compressive strength before and after immersion in SBF, measured as the peak value for the initial 33% of compression. (C) Water absorption after immersion in SBF. (D) Mass loss after immersion in SBF. Error bars in all graphs show standard deviations.

layer was visible on the glass surface. For coated scaffolds, the CaP layer primarily appeared on the polymer surface, with little CaP on the glass beneath the coating. This was clearly seen also in areas where the coating had detached from the glass surface: the CaP layer had mainly formed on the coating and to a lesser extent on the glass surface. The SEM images did not reveal any clear differences between the CaP layer on the different coatings.

The SBF solution was replenished weekly to simulate in vivo conditions in which released ions do not accumulate in the surrounding fluid over time. During the first 3 weeks, the pH values for the immersion solutions of all scaffolds were elevated due to the ion exchange reactions occurring on the bioactive glass surface (Figure 7). At weeks 1 and 2, the pH of the immersion solution of the uncoated scaffolds was significantly higher than that of coated scaffolds ($p < .005$). After the initial 3 weeks, pH values approached that of fresh SBF (7.4 at 37°C).

Figure 5C presents the water absorption of uncoated and coated scaffolds. The water absorption of uncoated scaffolds and PDLLA- and PLLA-coated scaffolds was between 5% and 11% at all time points with no differences between the coatings. In contrast, the water absorption of PLA SC scaffolds was significantly higher at all time points, with average values ranging from 12% to 15%. From the 2-week to 10-week time points, water absorption remained unchanged for all scaffold groups.

Mass loss for all scaffolds was small over the 10-week immersion time (Figure 5D). Uncoated scaffolds experienced the greatest mass

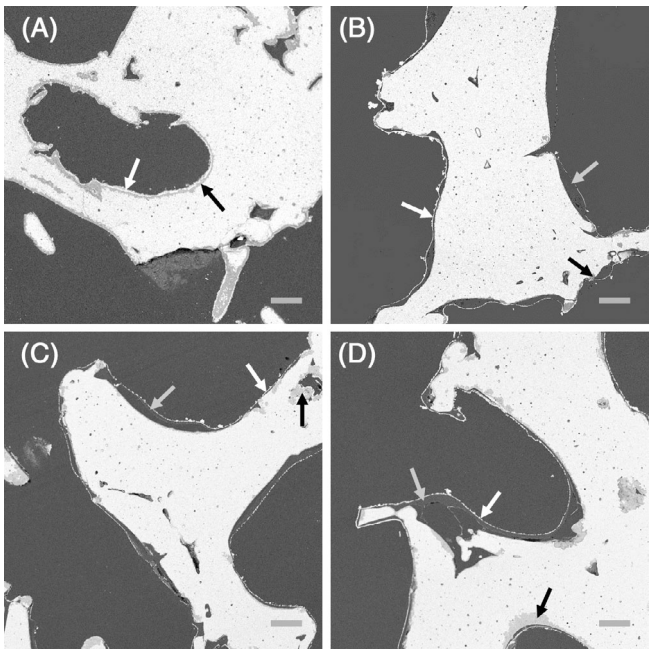

FIGURE 6 Cross-sectional SEM images of 10-week scaffolds: (A) uncoated, (B) PDLLA coating, (C) PLLA coating, and (D) PLA SC coating. Arrows indicate silica-rich layer (black arrow), CaP layer (white arrow), and PLA coating (gray arrow). Scale bar = 200 μm. PDLLA, amorphous poly(D,L-lactide); PLA, polylactide; PLLA, poly(L-lactide); PLA SC, polylactide stereocomplexes.

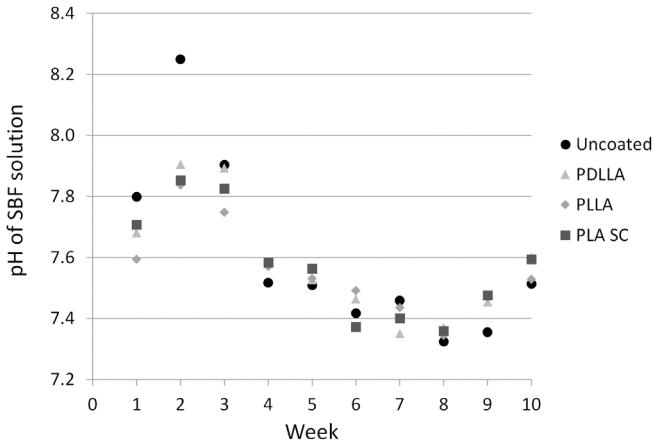

FIGURE 7 pH values of simulated body fluid (SBF) solution of uncoated and coated bioactive glass scaffolds. Immersion solutions were replenished weekly to fresh SBF and deviations from pH 7.4 are not cumulative. A total of 214 pH measurements were conducted for all scaffolds, with a standard deviation of ±0.16 between parallel samples.

loss at all time points, significantly differing from coated scaffolds ($p = .014$). After each immersion time, mass loss of PDLLA scaffolds was higher than that of PLLA ($p = .0027$) and PLA SC ($p = .024$) scaffolds. No statistically significant difference was found between PLLA and PLA SC ($p = .20$).

4 | DISCUSSION

The tensile properties of PLA SC have been reported by several authors,[27–31] but its compressive properties require further investigation. In this study, we used PLAs with varying stereocompositions as coatings for bioactive glass scaffolds in a clinically relevant bone regeneration setting. We compared the mechanical and short-term degradation properties of amorphous PDLLA, homocrystalline PLLA, and a mixture of PLLA and PDLA that resulted in stereocomplex crystallinity.

Compressive testing results showed significantly higher toughness and strength for PLA-coated scaffolds than for uncoated scaffolds. In the dry state before immersion in SBF, toughness differed approximately fourfold, and in the wet state after immersion, by approximately twofold. As the properties of uncoated scaffolds remained unchanged from dry to wet states, the observed differences in the coated scaffolds can be attributed to changes in the coating. PLA is a slowly degrading polymer,[54] and most changes in mechanical properties during the study timeframe can probably be explained by the plasticizing effect of water absorption into the polymer.[55] Additionally, scaffold wetting may have affected the adherence of the coating to the glass surface.

Scaffolds with semi-crystalline coating (PLLA and PLA SC) displayed greater toughness than those with amorphous coatings (PDLLA). Although PLA SC averages were higher than PLLA, there was no statistically significant difference between them. Earlier studies have shown PLA SC tensile strength to be similar or higher than that of isomerically pure PLLA, but wide variations in elongation-at-break have been recorded, with values for PLA SC both above and below PLLA.[27–31] More detailed studies should be conducted to determine the influence of factors such as crystal structure, percent crystallinity, and molecular weight on the mechanical properties of PLA SC compared to optically pure PLA.

It is crucial to optimize the mechanical properties of scaffolds for tissue regeneration to ensure that they are suitable for the surgical procedure. Surgically treated bone defects are often stabilized using intramedullary nails, screwed plates, or external fixators.[56] Even bone void fillers with lower mechanical properties may be utilized for the regeneration of load-bearing bone tissue, especially when the load is supported by the fixation devices.[57,58] In this study, the physical handling characteristics of coated scaffolds were improved compared to uncoated scaffolds, which were brittle and prone to breaking during experimental preparation.

Highly porous glass scaffolds were prepared using the template sintering technique. While creating glass scaffolds with lower overall porosity or smaller pore size could have significantly increased compressive strength,[48] it might have reduced their suitability for bone regeneration within the scaffold. Longer sintering times or higher sintering temperatures could have enhanced the compressive properties of the glass scaffolds by densifying the struts.[59] Additionally, a thicker coating or using a higher molecular weight polymer for the coating could have resulted in higher compressive properties. The compressive properties of the scaffolds analyzed in this study were comparable to previously reported values for polymer-coated, template-sintered scaffolds.[49,60]

The immersion solution was refreshed with new SBF weekly, allowing the measured pH values to reflect reactions that occurred during the previous week. The rate of ion exchange reactions in the bioactive glass was high during the first 3 weeks of immersion, resulting in increased pH values and mass loss of the scaffolds. The peak pH values were lower for coated scaffolds than for uncoated scaffolds. A pronounced pH peak immediately after immersion of bioactive glass into an aqueous solution has been reported to contribute to its antimicrobial effect.[61–63] However, an increase in pH can negatively impact cellular activity and potentially cause cytotoxic effects to the surrounding tissue.[64,65] It may therefore be beneficial to moderate the initial pH peak for example using coatings, such as those used in the present study. A slight increase in pH has been shown to positively influence osteoblast activity and contribute to new bone formation.[66,67] Throughout this study, differences between the PLA coatings were small. These findings are consistent with the results in an earlier study, where minor differences in pH were observed between films containing PLLA or a mixture of PLLA and PDLA during immersion at 37°C in a buffered solution for up to 39 weeks.[18]

The amorphous CaP layer that forms on bioactive glass progressively crystallizes into hydroxyapatite, promoting protein adsorption, cell attachment and differentiation, and new bone formation.[68] In this study, a CaP layer formed also on the surface of the PLA coating,

indicating that bone growth could be facilitated on the polymer surface similarly to uncoated bioactive glass. This phenomenon has been previously reported and is considered important for bone regeneration potential.[69–72]

Throughout the 10-week immersion period in SBF, mass loss of the scaffolds was small. Uncoated scaffolds consistently experienced the greatest mass loss, indicating that the coating prevented mass loss from the glass. However, the differences were small. Bioactive glass 13–93 is a slowly dissolving glass, and the rate of dissolution fits earlier reported data well.[73,74] The long degradation time of PLA also contributed to the limited mass loss observed in the scaffolds during the 10-week immersion.

DSC analysis revealed a high degree of stereocomplexation in PLA SC coatings, evidenced by the absence of homocrystal melting peaks for most PLA SC scaffolds. However, precise crystallinity measurements were unattainable, as bioactive glass present in the samples obscured the individual polymer masses. The T_g values of both PLLA and PLA SC were relatively high. For instance, the T_g value of 68°C for PLLA in both 0-week and 10-week scaffolds exceeded typical T_g values for PLA[11] but remained within the reported range.[75] The higher T_g values may result from the annealing process that was performed after scaffold coating. Comparable T_g values have been obtained by annealing[76–78] and physical aging at 40°C.[79] The 4°C T_g increase observed in PLA SC during the 10-week immersion in SBF may have resulted from volume relaxation leading to reduced segmental mobility of the polymer.[80] Conversely, the appearance of a crystallization peak at approximately 93°C for 10-week PLLA scaffolds may have resulted from increased polymer chain mobility caused by chain scission, resulting in a higher probability for crystal formation. Hydrolysis typically causes the degradation of amorphous regions first, increasing the mobility of undegraded chain segments and increasing crystallization potential.[81] These different behaviors may result from slower degradation of PLA SC compared to homocrystalline PLLA.[14] The T_m decrease of PLLA during hydrolysis and the unchanged T_m of stereocomplex crystallites have been reported previously.[14,82]

5 | CONCLUSIONS

We manufactured porous coated and uncoated bioactive glass scaffolds with potential applications in bone regeneration. Scaffolds with a PLA coating showed higher toughness than uncoated glass scaffolds, with an approximately fourfold increase in dry state and a twofold increase in wet state after up to 10-week immersion in SBF. Homocrystalline PLLA and stereocomplex PLA SC coatings had the highest average toughness with a significant difference to the amorphous PDLLA coating after immersion. Crucially, all coatings improved the handling characteristics of the scaffolds, which is essential for their potential clinical use.

CaP precipitation and subsequent hydroxyapatite formation are key indicators of glass bioactivity and important for cell attachment to scaffold surfaces. In our study, a CaP layer formed on the surface of all scaffolds after immersion in SBF. For uncoated scaffolds, the CaP layer was present on the glass surface, while for coated scaffolds, it had primarily formed on the surface of the PLA coating. Notably, the polymeric coating effectively moderated the initial potentially cytotoxic pH peak originating from the surface reactions of the bioactive glass.

Our findings indicate that the properties of bioactive glass scaffolds can be significantly enhanced using thin PLA-based coatings. In addition, using PLA stereocomplexes as coatings may offer additional benefits by increasing the overall toughness of the scaffold structure.

ACKNOWLEDGMENTS

The authors would like to thank Sara Kiran for her work on the foam replication method to produce glass scaffolds. We would also like to thank Dr. Tiina Saloranta-Simell for assistance with freeze drying, Jarl Hemming with the GPC measurements and Linus Silvander for the SEM analyses. Peter Uppstu is grateful for financial support from The Finnish Foundation of Technology Promotion, The Swedish Cultural Foundation in Finland, and the Åbo Akademi University Foundation.

DATA AVAILABILITY STATEMENT

Research data are not shared.

ORCID

Peter Uppstu https://orcid.org/0000-0002-6447-3355
Simon Engblom https://orcid.org/0000-0002-6460-5186
Leena Hupa https://orcid.org/0000-0001-7745-7779
Carl-Eric Wilén https://orcid.org/0000-0001-7720-3234

REFERENCES

1. Puppi D, Chiellini F, Piras AM, Chiellini E. Polymeric materials for bone and cartilage repair. *Prog Polym Sci*. 2010;35:403-440.
2. Lee S, Shin H. Matrices and scaffolds for delivery of bioactive molecules in bone and cartilage tissue engineering. *Adv Drug Deliv Rev*. 2007;59:339-359.
3. Tian H, Tang Z, Zhuang X, Chen X, Jing X. Biodegradable synthetic polymers: preparation, functionalization and biomedical application. *Prog Polym Sci*. 2012;37:237-280.
4. Tajbakhsh S, Hajiali F. A comprehensive study on the fabrication and properties of biocomposites of poly(lactic acid)/ceramics for bone tissue engineering. *Mater Sci Eng C*. 2017;70:897-912.
5. Lasprilla AJR, Martinez GAR, Lunelli BH, Jardini AL, Filho RM. Poly-lactic acid synthesis for application in biomedical devices — a review. *Biotechnol Adv*. 2012;30:321-328.
6. Narayanan G, Vernekar VN, Kuyinu EL, Laurencin CT. Poly (lactic acid)-based biomaterials for orthopaedic regenerative engineering. *Adv Drug Deliv Rev*. 2016;107:247-276.
7. Inkinen S, Hakkarainen M, Albertsson A, Sodergard A. From lactic acid to poly(lactic acid) (PLA): characterization and analysis of PLA and its precursors. *Biomacromolecules*. 2011;12:523-532.
8. Farah S, Anderson DG, Langer R. Physical and mechanical properties of PLA, and their functions in widespread applications—a comprehensive review. *Adv Drug Deliv Rev*. 2016;107:367-392.
9. Rahaman MH, Tsuji H. Synthesis and characterization of stereo multiblock poly(lactic acid)s with different block lengths by melt polycondensation of poly(L-lactic acid)/poly(D-lactic acid) blends. *Macromol React Eng*. 2012;6:446-457.
10. de Jong SJ, van Dijk-Wolthuis WNE, Kettenes-van dB, Schuyl PJW, Hennink WE. Monodisperse enantiomeric lactic acid oligomers:

preparation, characterization, and stereocomplex formation. *Macromolecules*. 1998;31:6397-6402.
11. Tsuji H. Poly(lactide) stereocomplexes: formation, structure, properties, degradation, and applications. *Macromol Biosci*. 2005;5:569-597.
12. Kakuta M, Hirata M, Kimura Y. Stereoblock polylactides as high-performance bio-based polymers. *Polym Rev*. 2009;49:107-140.
13. Bouapao L, Tsuji H. Stereocomplex crystallization and spherulite growth of low molecular weight poly(L-lactide) and poly(D-lactide) from the melt. *Macromol Chem Phys*. 2009;210:993-1002.
14. Tsuji H. In vitro hydrolysis of blends from enantiomeric poly(lactide)s. Part 1. Well-stereo-complexed blend and non-blended films. *Polymer*. 2000;41:3621-3630.
15. Tsuji H. In vitro hydrolysis of blends from enantiomeric poly(lactide)s. Part 4: well-homo-crystallized blend and nonblended films. *Biomaterials*. 2003;24:537-547.
16. Regnell Andersson S, Hakkarainen M, Inkinen S, Södergård A, Albertsson A. Customizing the hydrolytic degradation rate of stereocomplex PLA through different PDLA architectures. *Biomacromolecules*. 2012;13:1212-1222.
17. Tsuji H, Fukui I. Enhanced thermal stability of poly(lactide)s in the melt by enantiomeric polymer blending. *Polymer*. 2003;44:2891-2896.
18. Andersson SR, Hakkarainen M, Inkinen S, Södergård A, Albertsson A. Polylactide stereocomplexation leads to higher hydrolytic stability but more acidic hydrolysis product pattern. *Biomacromolecules*. 2010;11:1067-1073.
19. Haaparanta A, Uppstu P, Hannula M, Ellä V, Rosling A, Kellomäki M. Improved dimensional stability with bioactive glass fibre skeleton in poly(lactide-co-glycolide) porous scaffolds for tissue engineering. *Mater Sci Eng C*. 2015;56:457-466.
20. Uppstu P, Paakki C, Rosling A. In vitro hydrolysis and magnesium release of poly(d,l-lactide-co-glycolide)-based composites containing bioresorbable glasses and magnesium hydroxide. *J Appl Polym Sci*. 2015;132:42646.
21. Björkenheim R, Strömberg G, Ainola M, et al. Bone morphogenic protein expression and bone formation are induced by bioactive glass S53P4 scaffolds in vivo. *J Biomed Mater Res*. 2019;107:847-857.
22. Björkenheim R, Strömberg G, Pajarinen J, et al. Polymer-coated bioactive glass S53P4 increases VEGF and TNF expression in an induced membrane model in vivo. *J Mater Sci*. 2017;52:9055-9065.
23. Björkenheim R, Jämsen E, Eriksson E, et al. Sintered S53P4 bioactive glass scaffolds have anti-inflammatory properties and stimulate osteogenesis in vitro. *Eur Cell Mater*. 2021;41:15-30.
24. Eriksson E, Björkenheim R, Strömberg G, et al. S53P4 bioactive glass scaffolds induce BMP expression and integrative bone formation in a critical-sized diaphysis defect treated with a single-staged induced membrane technique. *Acta Biomater*. 2021;126:463-476.
25. Fukushima K, Kimura Y. Stereocomplexed polylactides (Neo-PLA) as high-performance bio-based polymers: their formation, properties, and application. *Polym Int*. 2006;55:626-642.
26. Garlotta D. A literature review of poly(lactic acid). *J Polym Environ*. 2001;9:63-84.
27. Tsuji H, Ikada Y. Stereocomplex formation between enantiomeric poly(lactic acid)s. XI. Mechanical properties and morphology of solution-cast films. *Polymer*. 1999;40:6699-6708.
28. López-Rodríguez N, Martínez de Arenaza I, Meaurio E, Sarasua JR. Improvement of toughness by stereocomplex crystal formation in optically pure polylactides of high molecular weight. *J Mech Behav Biomed Mater*. 2014;37:219-225.
29. Sarasua JR, Arraiza AL, Balerdi P, Maiza I. Crystallinity and mechanical properties of optically pure polylactides and their blends. *Polym Eng Sci*. 2005;45:745-753.
30. Takasaki M, Ito H, Kikutani T. Development of stereocomplex crystal of polylactide in high-speed melt spinning and subsequent drawing and annealing processes. *J Macromol Sci B*. 2003;42:403-420.
31. Furuhashi Y, Kimura Y, Yoshie N, Yamane H. Higher-order structures and mechanical properties of stereocomplex-type poly(lactic acid) melt spun fibers. *Polymer*. 2006;47:5965-5972.
32. Yan Z, Liao X, He G, et al. Green and high-expansion PLLA/PDLA foams with excellent thermal insulation and enhanced compressive properties. *Ind Eng Chem Res*. 2020;59:19244-19251.
33. Li W, Ren Q, Zhu X, et al. Enhanced heat resistance and compression strength of microcellular poly (lactic acid) foam by promoted stereocomplex crystallization with added D-mannitol. *J CO2 Util*. 2022;63:102118.
34. Cui W, Wei X, Luo J, Xu B, Zhou H, Wang X. CO2-assisted fabrication of PLA foams with exceptional compressive property and heat resistance via introducing well-dispersed stereocomplex crystallites. *J CO2 Util*. 2022;64:102184.
35. van Gestel NAP, Geurts J, Hulsen DJW, van Rietbergen B, Hofmann S, Arts JJ. Clinical applications of S53P4 bioactive glass in bone healing and osteomyelitic treatment: a literature review. *Biomed Res Int*. 2015;2015:684826.
36. Hench LL. Chronology of bioactive glass development and clinical applications. *New J Glass Ceram*. 2013;3:67-73.
37. Baino F, Hamzehlou S, Kargozar S. Bioactive glasses: where are we and where are we going? *J Funct Biomater*. 2018;9:25.
38. Fagerlund S, Massera J, Moritz N, Hupa L, Hupa M. Phase composition and in vitro bioactivity of porous implants made of bioactive glass S53P4. *Acta Biomater*. 2012;8:2331-2339.
39. Ylänen H, Karlsson KH, Itälä A, Aro HT. Effect of immersion in SBF on porous bioactive bodies made by sintering bioactive glass microspheres. *J Non Cryst Solids*. 2000;275:107-115.
40. Huang TS, Rahaman MN, Doiphode ND, et al. Porous and strong bioactive glass (13–93) scaffolds fabricated by freeze extrusion technique. *Mater Sci Eng C*. 2011;31:1482-1489.
41. Kolan KCR, Leu MC, Hilmas GE, Brown RF, Velez M. Fabrication of 13-93 bioactive glass scaffolds for bone tissue engineering using indirect selective laser sintering. *Biofabrication*. 2011;3:025004.
42. Chen QZ, Thompson ID, Boccaccini AR. 45S5 Bioglass®-derived glass–ceramic scaffolds for bone tissue engineering. *Biomaterials*. 2006;27:2414-2425.
43. Brink M. The influence of alkali and alkaline earths on the working range for bioactive glasses. *J Biomed Mater Res Part B: Appl Biomater*. 1997;36:109-117.
44. Fagerlund S, Massera J, Hupa M, Hupa L. T–T–T behaviour of bioactive glasses 1–98 and 13–93. *J Eur Ceram Soc*. 2012;32:2731-2738.
45. Brown RF, Day DE, Day TE, Jung S, Rahaman MN, Fu Q. Growth and differentiation of osteoblastic cells on 13–93 bioactive glass fibers and scaffolds. *Acta Biomater*. 2008;4:387-396.
46. Rezwan K, Chen QZ, Blaker JJ, Boccaccini AR. Biodegradable and bioactive porous polymer/inorganic composite scaffolds for bone tissue engineering. *Biomaterials*. 2006;27:3413-3431.
47. Fu Q, Saiz E, Rahaman MN, Tomsia AP. Bioactive glass scaffolds for bone tissue engineering: state of the art and future perspectives. *Mater Sci Eng C*. 2011;31:1245-1256.
48. Gerhardt L, Boccaccini AR. Bioactive glass and glass-ceramic scaffolds for bone tissue engineering. *Materials*. 2010;3:3.
49. Philippart A, Boccaccini AR, Fleck C, Schubert DW, Roether JA. Toughening and functionalization of bioactive ceramic and glass bone scaffolds by biopolymer coatings and infiltration: a review of the last 5 years. *Expert Rev Med Devices*. 2015;12:93-111.
50. Mohamad Yunos D, Bretcanu O, Boccaccini AR. Polymer-bioceramic composites for tissue engineering scaffolds. *J Mater Sci*. 2008;43:4433-4442.
51. Rahaman MN, Wei X, Wenhai H. Review—bioactive glass implants for potential application in structural bone repair. *Biomed Glass*. 2017;3:56.

52. Kokubo T, Kushitani H, Sakka S, Kitsugi T, Yamamuro T. Solutions able to reproduce in vivo surface-structure changes in bioactive glass-ceramic A-W3. *J Biomed Mater Res*. 1990;24:721-734.
53. Tsuji H. Poly(lactic acid) stereocomplexes: a decade of progress. *Adv Drug Deliv Rev*. 2016;107:97-135.
54. Danoux CB, Barbieri D, Yuan H, de Bruijn J, van Blitterswijk CA, Habibovic P. In vitro and in vivo bioactivity assessment of a polylactic acid/hydroxyapatite composite for bone regeneration. *Biomatter*. 2014;4:e27664.
55. Redondo FL, Giaroli MC, Ciolino AE, Ninago MD. Preparation of porous poly(lactic acid)/tricalcium phosphate composite scaffolds for tissue engineering. *Biointerface Res Appl Chem*. 2022;12:5610-5624.
56. Nieto H, Baroan C. Limits of internal fixation in long-bone fracture. *Orthop Traumatol Surg Res*. 2017;103:S61-S66.
57. Auregan J-C, Begue T. Induced membrane for treatment of critical sized bone defect: a review of experimental and clinical experiences. *Int Orthop*. 2014;38:1971-1978.
58. Bongio M, van den Beucken JJJP, Leeuwenburgh SCG, Jansen JJ. Development of bone substitute materials: from 'biocompatible' to 'instructive'. *J Mater Chem*. 2010;20:8747-8759.
59. Eqtesadi S, Motealleh A, Miranda P, Pajares A, Lemos A, Ferreira JMF. Robocasting of 45S5 bioactive glass scaffolds for bone tissue engineering. *J Eur Ceram Soc*. 2014;34:107-118.
60. Fiume E, Ciavattini S, Verné E, Baino F. Foam replica method in the manufacturing of bioactive glass scaffolds: out-of-date technology or still underexploited potential? *Materials*. 2021;14:2795.
61. Zhang D, Leppäranta O, Munukka E, et al. Antibacterial effects and dissolution behavior of six bioactive glasses. *J Biomed Mater Res*. 2010;93A:475-483.
62. Drago L, Toscano M, Bottagisio M. Recent evidence on bioactive glass antimicrobial and antibiofilm activity: a mini-review. *Materials*. 2018;2:11.
63. Stoor P, Söderling E, Salonen JI. Antibacterial effects of a bioactive glass paste on oral microorganisms. *Acta Odontol Scand*. 1998;56:161-165.
64. El-Ghannam A, Ducheyne P, Shapiro IM. Formation of surface reaction products on bioactive glass and their effects on the expression of the osteoblastic phenotype and the deposition of mineralized extracellular matrix. *Biomaterials*. 1997;18:295-303.
65. El-Rashidy AA, Roether JA, Harhaus L, Kneser U, Boccaccini AR. Regenerating bone with bioactive glass scaffolds: a review of in vivo studies in bone defect models. *Acta Biomater*. 2017;62:1-28.
66. Kaysinger KK, Ramp WK. Extracellular pH modulates the activity of cultured human osteoblasts. *J Cell Biochem*. 1998;68:83-89.
67. Arnett TR. Extracellular pH Regulates Bone Cell Function. *J Nutr*. 2008;138:415S-418S.
68. Jones JR. Review of bioactive glass: from Hench to hybrids. *Acta Biomater*. 2013;9:4457-4486.
69. Wang X, Zhang Molino B, Pitkänen S, et al. 3D scaffolds of polycaprolactone/copper-doped bioactive glass: architecture engineering with additive manufacturing and cellular assessments in a coculture of bone marrow stem cells and endothelial cells. *ACS Biomater Sci Eng*. 2019;5:4496-4510.
70. Oudadesse H, Najem S, Mosbahi S, et al. Development of hybrid scaffold: bioactive glass nanoparticles/chitosan for tissue engineering applications. *J Biomed Mater Res Part A*. 2020;109:590-599.
71. Bochicchio B, Barbaro K, De Bonis A, Rau JV, Pepe A. Electrospun poly(D,L-lactide)/gelatin/glass-ceramics tricomponent nanofibrous scaffold for bone tissue engineering. *J Biomed Mater Res Part A*. 2020;108:1064-1076.
72. Plyusnin A, Kulkova J, Arthurs G, Jalava N, Uppstu P, Moritz N. Biological response to an experimental implant for tibial tuberosity advancement in dogs: a pre-clinical study. *Res Vet Sci*. 2020;128:183-196.
73. Nommeots-Nomm A, Labbaf S, Devlin A, et al. Highly degradable porous melt-derived bioactive glass foam scaffolds for bone regeneration. *Acta Biomater*. 2017;57:449-461.
74. Sinitsyna P, Karlström O, Sevonius C, Hupa L. In vitro dissolution and characterisation of flame-sprayed bioactive glass microspheres S53P4 and 13–93. *J Non Cryst Solids*. 2022;591:121736.
75. Madhavan Nampoothiri K, Nair NR, John RP. An overview of the recent developments in polylactide (PLA) research. *Bioresour Technol*. 2010;101:8493-8501.
76. Park S, Todo M, Arakawa K. Effect of annealing on the fracture toughness of poly(lactic acid). *J Mater Sci*. 2004;39:1113-1116.
77. Tábi T, Sajó IE, Szabó F, Luyt AS, Kovács JG. Crystalline structure of annealed polylactic acid and its relation to processing. *Express Polym Lett*. 2010;4:659-668.
78. Dong T, Yu Z, Wu J, et al. Thermal and barrier properties of stretched and annealed polylactide films. *Polym Sci Ser A*. 2015;57:738-746.
79. Pan P, Zhu B, Inoue Y. Enthalpy relaxation and embrittlement of poly(l-lactide) during physical aging. *Macromolecules*. 2007;40:9664-9671.
80. Bergström J, Hayman D. An overview of mechanical properties and material modeling of polylactide (PLA) for medical applications. *Ann Biomed Eng*. 2016;44:330-340.
81. Södergård A, Stolt M. Properties of lactic acid based polymers and their correlation with composition. *Prog Polym Sci*. 2002;27:1123-1163.
82. Pekarek Leach KJ, Mathiowitz E. Degradation of double-walled polymer microspheres of PLLA and P(CPP:SA)20:80. I In vitro degradation. *Biomaterials*. 1998;19:1973-1980.

How to cite this article: Uppstu P, Engblom S, Inkinen S, Hupa L, Wilén C-E. Influence of polylactide coating stereochemistry on mechanical and in vitro degradation properties of porous bioactive glass scaffolds for bone regeneration. *J Biomed Mater Res*. 2023;1-10. doi:10.1002/jbm.b.35328